

T. Y. Cho  
B. Heck  
G. Strobl

## Equations describing lamellar structure parameters and melting points of polyethylene-*co*-(butene/octene)s

Received: 16 February 2004  
Accepted: 17 March 2004  
Published online: 29 April 2004  
© Springer-Verlag 2004

B. Heck · G. Strobl  
Physikalisches Institut,  
Albert-Ludwigs-Universität,  
79104 Freiburg, Germany

T. Y. Cho (✉)  
School of Chemistry,  
Seoul National University,  
Seoul, Korea  
E-mail: tai-yon@psl.snu.ac.kr

**Abstract** Time- and temperature-dependent SAXS-experiments were used to determine the effect of octene and butene co-units on the lamellar structure and the melting properties of polyethylene. As expected, melting points decrease with increasing co-unit content, but crystal thicknesses are not affected and depend on the crystallization temperature only. Results can be cast into some simple equations which describe the dependence:

1. Of the melting point  $T_f$  on the crystal thickness  $d_c$  and the co-unit content  $x_B$

2. Of the equilibrium melting point  $T_f^\infty$  on  $x_B$   
3. Of  $d_c$  on the crystallization temperature  $T_c$   
4. Of the long spacing  $L$  on  $T_c$ ,  $x_B$  and the molar mass  
5. Of  $T_f$  on  $T_c$ .

**Keywords** Equations · Lamellar structure parameters · Melting points · Octene · Butene · Polyethylene-*co*-(butene/octene)s

### Introduction

The introduction of co-units into a crystallizable stereoregular polymer chain generally reduces the crystallinity. The question arises how this occurs as a consequence of changes in the lamellar thickness  $d_c$  and in the packing density of the lamellae as described by the long spacing  $L$ . Conventional wisdom relates  $d_c$  with the supercooling below the equilibrium melting point of the copolymer. Since the equilibrium melting point surely decreases when the fraction  $x_B$  of co-units increases one expected for a fixed crystallization temperature  $T_c$  for increasing  $x_B$  a growth in the crystal thickness and—considering the decreasing crystallinity—an even larger growth of the long spacing. Surprising for many, this view turned out as being incorrect. A comprehensive investigation carried out by small-angle X-ray scattering (SAXS) for a syndiotactic polypropylene (sPP) and related octene

copolymers showed that the crystallite thickness at a fixed  $T_c$  is  $x_B$ -invariant [1]. The drop in the crystallinity with increasing  $x_B$  is therefore a result of a growth of  $L$  only. We also investigated polyethylene (PE)-derived copolymers, but for two samples only. The result was qualitatively similar to the sPP-system: at a fixed  $T_c$  we found—if any—only a minor difference in  $d_c$  [2].

Recently, we obtained a larger series of poly(ethylene-*co*-octene)s (P(E *co*O)) together with several poly(ethylene-*co*-butene)s (P(E *co*B)). All samples have similar molar masses, so that the co-unit content is the only varying property. We have now checked and further extended our previous limited studies on PE. The results are reported in the following. They lead us to the formulation of equations which describe the parameters of the lamellar structure and the related melting points in dependence on the crystallization temperature and the co-unit content.

## Experimental

**Samples** The experiments were carried out for a series of P(E *co*O)s and P(E *co*B)s which were kindly made available to us by Prof. Leo Mandelkern (Tallahassee, USA). Included in the studies was also a sample of linear polyethylene supplied by LG Chemicals, Daejeon, Korea. All samples are specified with their properties in Table 1.

The samples were crystallized isothermally at preset  $T_c$ s after a cooling from the melt at 150 °C. The kinetics of crystallization was analyzed by time-dependent SAXS experiments. After completion of the crystallization process samples were—in a second part of the experiment—heated up stepwise until complete melting. The structure variations during the heating were again followed by SAXS.

**SAXS** The SAXS experiments were carried out with the aid of a Kratky-camera attached to a conventional Cu- $K_\alpha$  X-ray source, employing a temperature controlled sample-holder. Using a position-sensitive metal wire detector, scattering curves were usually registered within a few minutes counting time. The slit-smeared data obtained were deconvoluted by application of an algorithm developed in our group [3]. Desmeared scattering curves were obtained in absolute values, as differential cross sections per unit volume,  $\Sigma(q)$ . With a knowledge of  $\Sigma(q)$  the one-dimensional electron density auto correlation function  $K(z)$  and its second derivative  $K''(z)$ , which gives the interface distance distribution function (IDF) [4, 5], can be directly calculated by applying the Fourier relations

$$K(z) = \frac{1}{r_e^2} \frac{1}{(2\pi)^3} \int_0^\infty \cos qz \cdot 4\pi q^2 \Sigma(q) dq \quad (1)$$

and

$$K''(z) = \frac{2}{r_e^2 (2\pi)^2} \int_0^\infty \left[ \lim_{q \rightarrow \infty} q^4 \Sigma(q) - q^4 \Sigma(q) \right] \cos qz dq \quad (2)$$

Here,  $q$  denotes the scattering vector  $q = 4\pi \sin \theta_B / \lambda$  ( $\theta_B$ : Bragg scattering angle);  $r_e$  is the classical electron radius.

A useful parameter in kinetic measurements and also the analysis of the continuous melting on heating is the

Porod coefficient  $P$ . It generally describes for two-phase systems the asymptotic behavior of the scattering curve as

$$\lim_{q \rightarrow \infty} \Sigma(q) = r_e^2 \frac{P}{(q/2\pi)^4} \quad (3)$$

The Porod coefficient is directly related to the interface area per unit volume,  $O_{ac}$ , by

$$P = \frac{1}{8\pi^3} O_{ac} (\rho_{e,c} - \rho_{e,a})^2 \quad (4)$$

whereby  $\rho_{e,c}$  and  $\rho_{e,a}$  denote the electron densities of the crystals and the fluid phase respectively. This relation is generally valid, for homogeneous as well as heterogeneous structures and therefore, for example, also if spherulites fill a sample only partially.

## Results

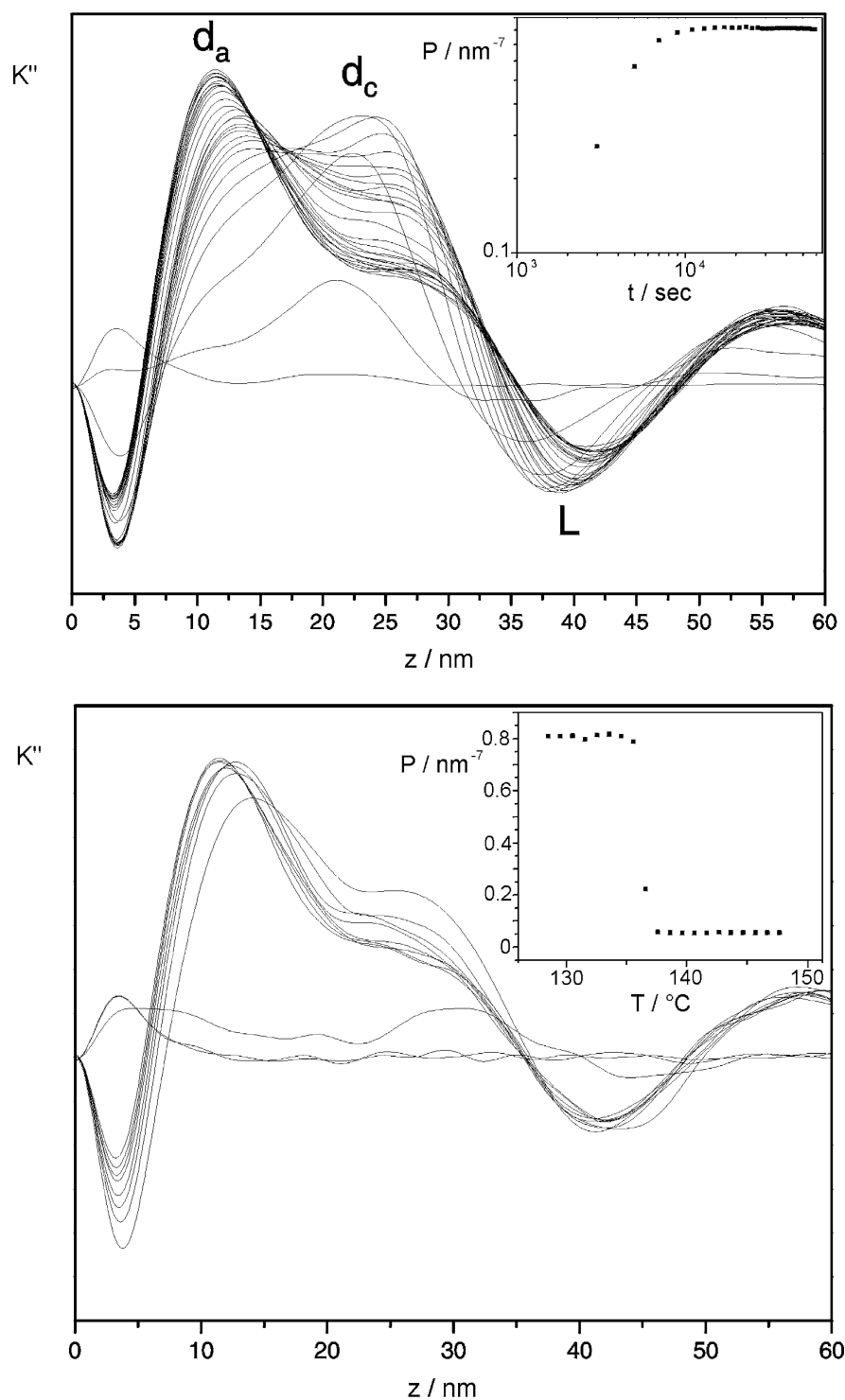
Figure 1 presents as one example for P(E *co*B(2.8%)) the IDFs derived from the SAXS curves measured both during an isothermal crystallization ( $T_c = 106$  °C) and a subsequent melting. The peak relates to the crystals, and its location gives their thickness,  $d_c = 6.2$  nm. The adjacent minimum yields the long spacing; alternatively  $L$  can also be derived from the location of the maximum of the Lorentz-corrected scattering intensity distribution  $Iq^2$ . One observes during the crystallization a fixed value of  $d_c$ , i.e., there is no crystal thickening. The temperature dependence of the Porod coefficient during the heating shown in the insert demonstrates that melting begins immediately above  $T_c$  and then continuously accelerates in rate. We derive the melting point, denoted  $T_f$ , in the same way as in a DSC-experiment, i.e., we associate it with the temperature where the rate of melting is at the maximum. This corresponds here to the temperature with the maximum slope in the curve  $P(T)$ . Note that the crystal thickness is also constant during the heating. The lower stability of the early-melting crystallites is therefore *not* due to a reduced thickness but to other factors, like the inner degree of order and the surroundings.

Quite different results are obtained for the LPE sample, as is shown in Fig. 2. The IDF here exhibits two peaks. The one at the lower value of  $z$  reflects the amorphous layers with a thickness  $d_a = 11$  nm, the other one, being located at the beginning of crystallization at  $z = 21$  nm, relates to the crystal thickness.  $d_c$  is obviously

**Table 1** Linear polyethylene, poly(ethylene-*co*-butene)s and poly(ethylene-*co*-octene)s used in the study

Sample	Linear PE	Ethylene-Butene		Ethylene-Octene		
Mw $\times 10^3$	60	100	101	105	71	85
Mw/Mn	2.9	2.0	2.0	2.0	2.1	2.2
Comonomer (mol%)	0.0	1.5	2.8	4.6	0.7	3.0
					92	2.3
					5.0	

**Fig. 1** P(EcoB(2.8%)): IDFs and Porod-coefficients derived from SAXS-curves obtained at different times during a crystallization at  $T_c = 106^\circ\text{C}$  (*top*) and at different temperatures during a subsequent heating up to the melt state (*bottom*). *Inserts* show the respective time- and temperature-dependent changes of the Porod-coefficient



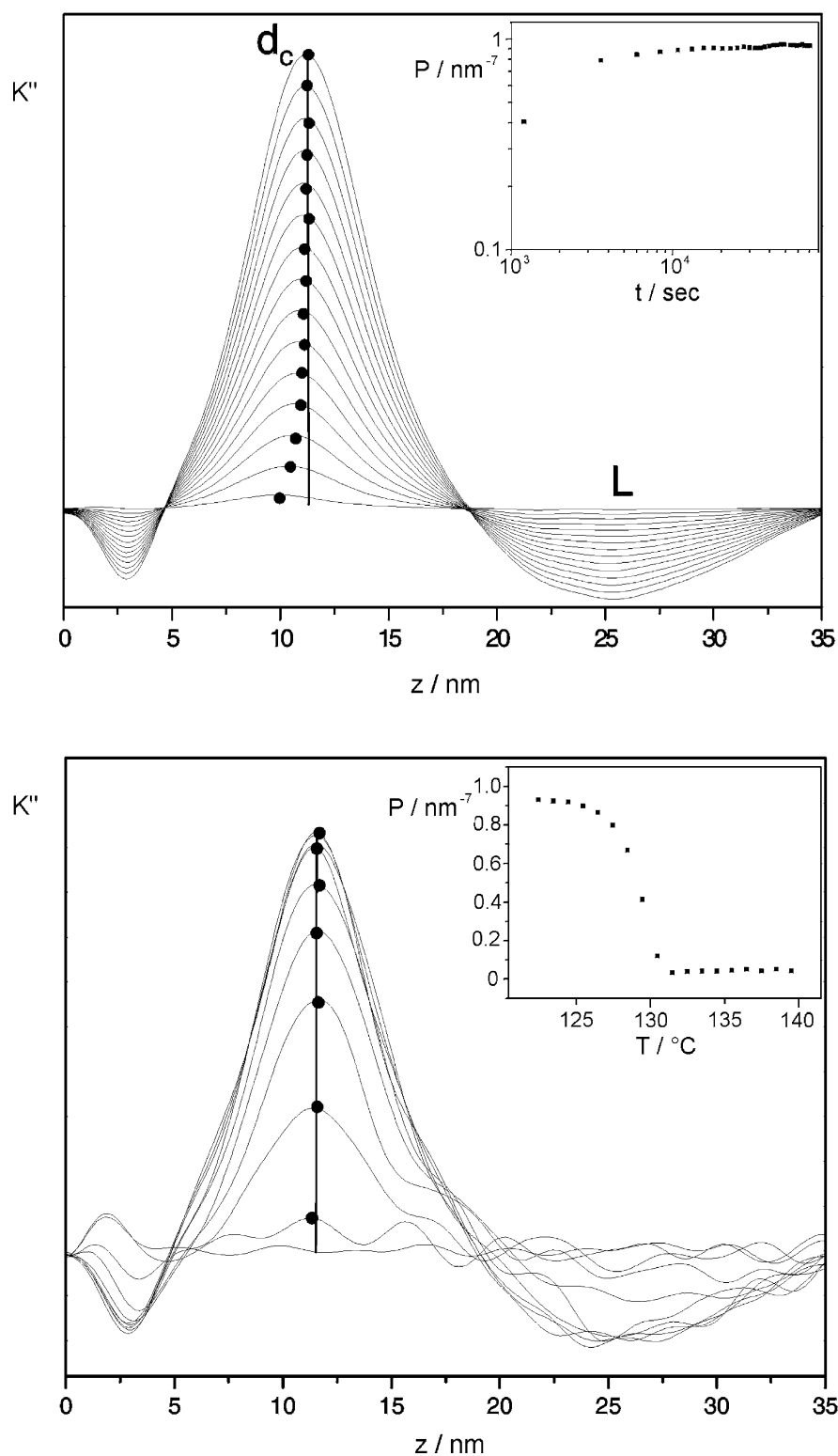
not constant during the isothermal crystallization but increases with time.

As a third example, Fig. 3 depicts the results obtained for a copolymer with a low co-unit content, P(EcoO(0.7%)). We observe again some change in  $d_c$  during

the isothermal crystallization, but it is smaller than for LPE.

The experiments provide for each chosen  $T_c$  the values of the crystal thickness  $d_c$  and the long spacing  $L$ . For the copolymers with  $x_B > 2\%$  these values are

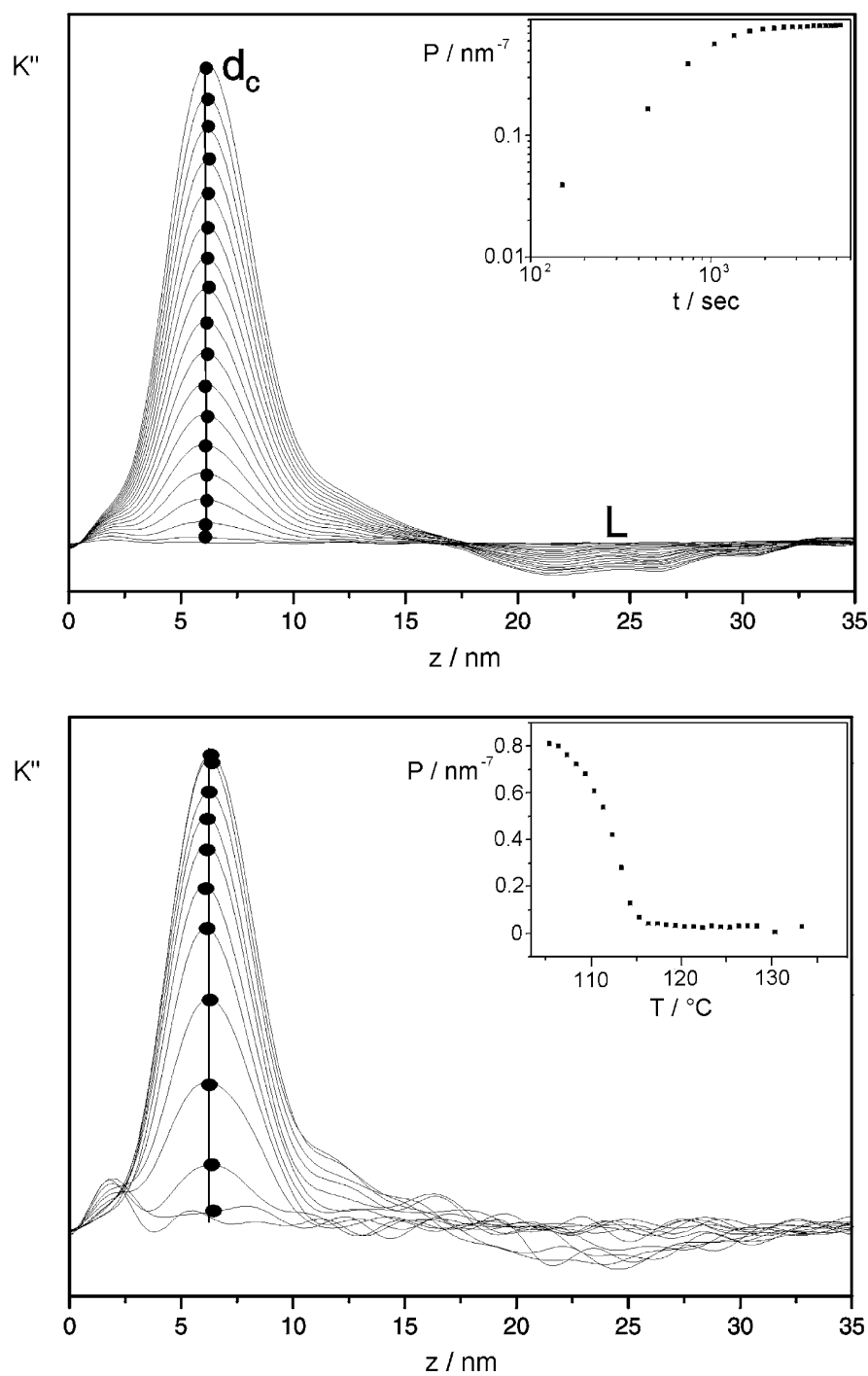
**Fig. 2** LPE: IDFs derived from SAXS-curves obtained at different times during a crystallization at  $T_c = 129^\circ\text{C}$  (*top*) and at different temperatures during a subsequent heating up to the melt state (*bottom*). The assignments of the peaks to  $d_a$ ,  $d_c$ , and  $L$  (thicknesses of amorphous layers and of crystallites, long spacing) are indicated



well-defined since thickening processes are absent. For the samples with lower co-unit content and LPE this is no longer the case. As a second result we can derive for all samples the melting points together with the

crystal thicknesses at  $T_f$ . The results thus obtained for all samples are presented together in Fig. 4. As suggested by the Gibbs-Thomson equation, the inverse thickness  $d_c^{-1}$  rather than  $d_c$  and, correspond-

**Fig. 3** P(E coO(0.7%)): IDFs and Porod-coefficients obtained during a crystallization at  $T_c = 123\text{ }^\circ\text{C}$  (*top*) and a subsequent heating into the melt state (*bottom*)



ingly,  $L^{-1}$  rather than  $L$  are chosen as variables. It can be seen that all the melting points can be allocated on a series of parallel “melting lines” with a downward shift for increasing  $x_B$ . In view of the limited accuracy no discrimination is made between LPE and P(E coO(0.7%)) or between P(E coO(2.8%)) and P(E coO(3%)); they are assembled on one common line respectively. The melting line for LPE extrapolates for

an infinite crystal thickness to  $141\text{ }^\circ\text{C}$ . This indeed is nearly identical with the equilibrium melting point of polyethylene,  $T_f^\infty(x_B = 0) = 141.4\text{ }^\circ\text{C}$ , as determined by Wunderlich in measurements on extended chain samples [6].

Different from the melting lines which vary with  $x_B$  one finds for the dependence  $d_c^{-1}(T_c)$  for all copolymers, both of the octene- and butene-type, for co-unit contents

above 2% a common, unique line. Deviations towards larger thickness values are only observed for a lower co-unit content and LPE, i.e., those samples which show a thickening during isothermal crystallization. When the “crystallization line” is linearly extrapolated to  $d_c^{-1} = 0$  it starts from the temperature  $T_c^\infty = 154^\circ\text{C}$ , i.e., clearly not from  $T_f^\infty(0)$ .

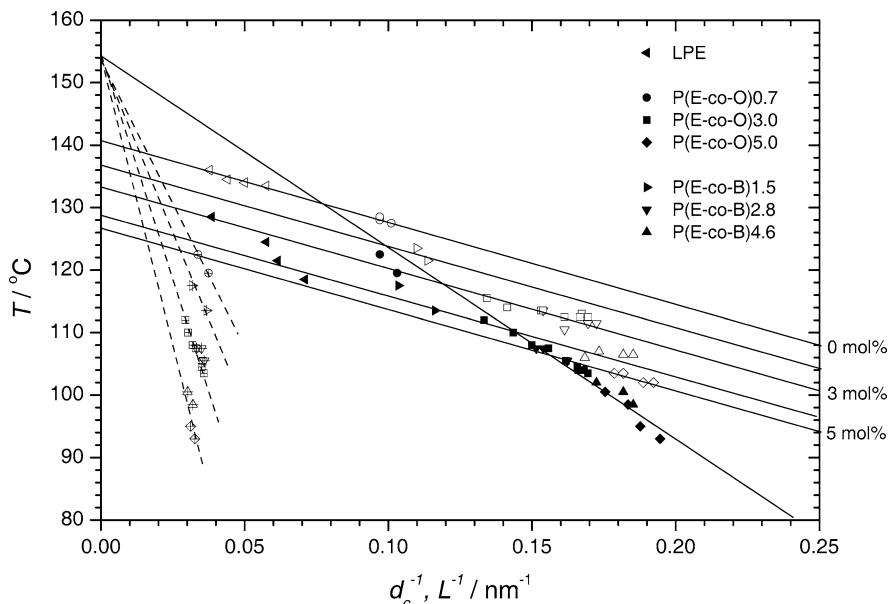
## Discussion

The results as presented in Fig. 4 confirm our first studies on PE and perfectly agree in the scenario with a general scheme first found for sPP and its copolymers. The invariance of  $d_c$  for samples with different co-unit content implies that the crystal thickness is *not* controlled by the supercooling below the respective melting point. Melting points decrease with increasing  $x_B$ , as is again demonstrated by the experiments, but the crystal thicknesses remain constant. Considering the appearance of the “crystallization line”  $T_c$  vs  $d_c^{-1}$ , it can be stated that  $d_c$  is indeed also determined by a supercooling, but one which refers to another specific temperature,  $T_c^\infty = 154^\circ\text{C}$ , which is located 13 K above the equilibrium melting point of PE.

In discussions of the melting point reduction by co-units often a simple result of Flory’s equilibrium theory is used. It states that the melting point reduction agrees with that introduced by a diluent with the same molar fraction, and is therefore also to be described by Raoult’s law, in the form

$$T_f^\infty(0) - T_f^\infty(x_B) = \frac{R[T_f^\infty(0)]^2}{\Delta h} x_B \quad (5)$$

**Fig. 4** Results of SAXS experiments on LPE, P(E coO)s and P(E coB)s. Crystal thicknesses and long spacings at the end of crystallizations at different temperatures, plotted as  $d_c^{-1}$  and  $L^{-1}$  vs  $T_c$  (filled and crossed symbols). Melting temperatures  $T_f$  and crystal thicknesses at  $T_f$  (open symbols). Representation of results using Gibbs-Thomson lines, one “crystallization line” for  $d_c^{-1}$  and four lines for  $L^{-1}$



where  $\Delta h$  denotes the heat of melting per mole of  $\text{C}_2\text{H}_4$ -groups. The results in Fig. 4 enable a check to be carried out. Figure 5 depicts the equilibrium melting points  $T_f^\infty(x_B)$  as given for the different samples by the limiting values of the Gibbs-Thomson lines for  $d_c^{-1} \rightarrow 0$ , in a comparison with Eq. (5). Non-negligible deviations are observed which increase with  $x_B$ . Such differences had already been found for the other investigated system, sPP and its copolymers, where they were even larger. Hence, treating copolymer systems by equilibrium thermodynamics does not seem to be of much value.

Figure 4 includes also values found for the long spacing. They are allocated on four different lines, one commonly for the copolymers with 4.6 and 5.0 mol% of co-units, one for 2.8 and 3.0 mol% of co-units, and the other two for 1.5 mol% and 0.7 mol% respectively. In the figure all lines start from  $T_c^\infty$  as the “crystallization line”. This choice implies that the linear crystallinity  $\phi_1 = d_c/L$  does not change with the crystallization temperature.

Such an invariance is, however, not found for the global crystallinity  $\phi$  as derived from the heat of fusion. For example, while the linear crystallinity of P(E coB(2.8%)) is always  $\phi_1 = 0.22 \pm 0.01$  the global crystallinity is  $\phi = 0.19, 0.16, 0.06$  for  $T_c = 104^\circ\text{C}, 106^\circ\text{C},$  and  $109^\circ\text{C}$  respectively.  $\phi$  is always smaller than  $\phi_1$  and decreases with increasing  $T_c$ . Where does this difference come from?  $\phi_1$  represents a geometric property, related to the short-range ordering of the crystal lamellae. If laterally extended lamellae would completely fill the sample volume one expects agreement between  $\phi_1$  and the global crystallinity  $\phi$ . This changes if the lateral extension is limited and distances arise between laterally adjacent lamellae. This seems to be the case here. The

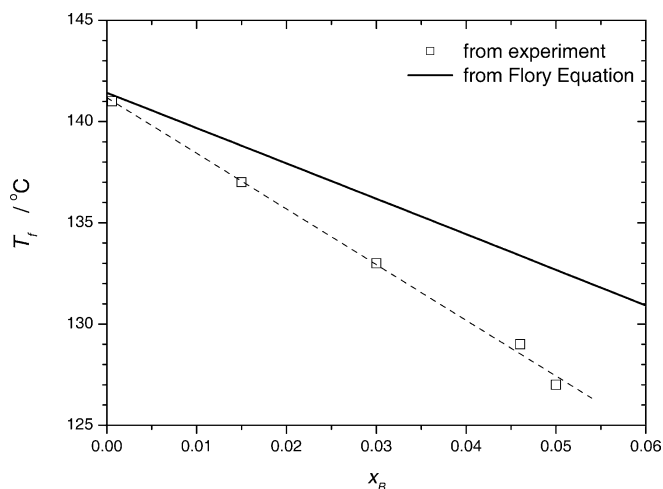


**Fig. 5** LPE, P(E coO)s, and P(E coB)s. Equilibrium melting points  $d_c^{-1}$  in dependence on the co-unit content, derived from the Gibbs-Thomson lines in Fig. 4. Comparison with Flory's equation (Eq. 5)

higher the crystallization temperature, the larger are these distances. For a higher  $T_c$  and correspondingly a higher  $d_c$  the growing lamellae become more selective with regard to the attachment of chain sequences between co-units. As it appears, the too short sequences, which cannot be included into the crystal and are therefore rejected, are not only placed in the interlamellar amorphous layers between the fold surfaces but increasingly also between adjacent lateral surfaces.

### Derived relationships

The results as given in Fig. 4 can be expressed by a number of equations. A first one is the specification of the Gibbs-Thomson relation for the investigated system. The melting lines in the figure relate the melting points of crystals in a copolymer melt to their thickness as

$$T_f = T_f^\infty(x_B) - \frac{C_1}{d_c} \quad (6)$$

with  $C_1 = 132 \text{ K nm}$

where  $C_1$  denotes the slope which is common to all the melting lines.  $T_f^\infty(x_B)$  is the limiting value of  $T_f$  for  $d_c^{-1} \rightarrow 0$ , where a macroscopic, co-unit free crystal is in equilibrium with the copolymer melt.  $T_f^\infty(x_B)$  thus represents the equilibrium crystallization/melting temperature of a copolymer with a volume fraction  $x_B$  of co-units. The Gibbs-Thomson relation gives for  $C_1$  the expression

$$C_1 = \frac{2\sigma_e T_f^\infty(0) \Delta z}{\Delta h} \quad (7)$$

Application of Eq. (7) yields for the surface free energy per endgroup,  $\sigma_e$ , the value  $5.0 \text{ kJ mol}^{-1}$ , choosing for

the molar heat of fusion per  $\text{C}_2\text{H}_4$ -group,  $\Delta h$ , the value  $293 \times 28 \text{ J mol}^{-1} = 8.2 \text{ kJ mol}^{-1}$ ;  $\Delta z$  is the length of a  $\text{C}_2\text{H}_4$ -unit in chain direction, equal to  $0.254 \text{ nm}$ .

The  $x_B$ -dependence of the equilibrium crystallization/melting temperature  $T_f^\infty(x_B)$  which is shown in Fig. 5 can be empirically described by the expression

$$\begin{aligned} T_f^\infty(x_B) &= T_f^\infty(0) - \alpha_1 x_B \\ \text{with } T_f^\infty(0) &= 141.2^\circ \text{C} \\ \alpha_1 &= 2.75 \times 10^2 \text{K} \end{aligned} \quad (8)$$

Here we use the exact value of the equilibrium crystallization/melting temperature of PE.

A particularly simple relationship holds for the crystal thickness  $d_c$ . In the absence of solid state thickening processes, which is given for not too low co-unit contents,  $d_c$  is independent of  $x_B$  and varies with  $T_c$  as described by the equation

$$\begin{aligned} d_c(T_c) &= \frac{C_2}{T_c^\infty - T_c} \\ \text{with } T_c^\infty &= 427 \text{K and } C_2 = 308 \text{K nm} \end{aligned} \quad (9)$$

The question about the origin of this relation is a primary one in the understanding of polymer crystallization. Our repeatedly expressed hypothetical answer [7] is: The "crystallization line" following from Eq. (9) when relating  $T_c$  to  $d_c^{-1}$  represents in the same manner as the Gibbs-Thomson line the locus of a thickness-dependent phase transition. Since the limiting temperature  $T_c^\infty$  definitely differs from the PE-equilibrium melting point  $T_c^\infty(0)$ , it cannot be a phase transition between the melt and the crystal, but must include an intermediate "mesomorphic" phase. The invariance of the line with regard to  $x_B$  would then mean that the co-units are already rejected when this mesomorphic phase forms out of the isotropic melt. There might exist other explanations, maybe quite different ones, but the experimental facts are obvious and speak clearly against a control of the structure formation process by the supercooling below the respective equilibrium melting point.

For the long spacing, we may formulate the equation

$$L(T_c, x_B) = \frac{\alpha_3(x_B)}{T_c^\infty - T_c} \quad (10)$$

which expresses a dependence on both, the crystallization temperature and the co-unit content. The observed  $x_B$ -dependence can be expressed in a linear approximation by

$$\alpha_3(x_B) = \alpha_4(1 + \alpha_5 x_B) \quad (11)$$

with

$$\alpha_4 = 0.8 \times 10^3 \text{K nm and } \alpha_5 = 26 \quad (12)$$

The long spacing is known to depend on the molar mass. In a work on PEEK Fougny et al. [8] have found that  $L$

changes with the degree of polymerization  $N$  in a way first suggested by Rault [9], namely similar to the radius of gyration as

$$L \sim N^{1/2} \quad (13)$$

The finding indicates that a given chain usually is included in one lamellae only. The simplest expression accounting for this dependence together with the  $x_B$ -dependence of Eq. (11) is

$$\alpha_3(x_B, N) = \alpha_6 N^{1/2} (1 + \alpha_5 x_B) \quad (14)$$

leading for the degree of polymerization of the series of samples,  $N \approx 3200$  ( $M \approx 90 \times 10^3$  g mol<sup>-1</sup>), to a parameter value

$$\alpha_6 = 14 \text{ K nm}$$

Finally, by combining the above equations it is possible to derive a relation between the crystallization temperature  $T_c$  and the subsequent melting point  $T_f$ , under the assumption of a complete absence of thickening and melting-recrystallization processes. As the SAXS experiments show, this is often the case for copolymers and is generally favored by high heating rates. One obtains

$$T_f(x_B, T_c) = T_f^\infty(x_B) - \frac{C_1}{C_2} (T_c^\infty - T_c) \quad (15)$$

and for the difference  $T_f(x_B, T_c) - T_c$  the expression

$$T_f(x_B, T_c) - T_c = T_f^\infty(x_B) - \frac{C_1}{C_2} T_c^\infty + T_c \left( \frac{C_1}{C_2} - 1 \right) \quad (16)$$

Introducing some of the numerical values leads to

$$T_f(x_B, T_c) - T_c = 231 \text{ K} - 231 x_B - 0.57 T_c \quad (17)$$

Note that the criterion

$$T_f(x_B, T_c) - T_c = 0$$

does *not* yield the equilibrium melting point as assumed in the popular Hoffmann-Weeks plot. The temperature where it is fulfilled, we denote it  $T_{cf}$ , represents—in our view—the crossover point from a pathway of polymer crystallization which uses an intermediate phase to a direct crystal formation out of the melt. Above  $T_{cf}$  the latter pathway, which requires a much longer time, remains the only available one. According to Fig. 4,  $T_{cf}$  varies with the co-unit content and reaches for LPE the highest value, located around 130 °C. Indeed, to our restricted knowledge, all  $T_c$ -dependent, isothermal crystallization experiments on LPE which started from a relaxed, quiescent melt end in temperature range 130–131 °C.

We expect the coefficients  $C_1$  and  $C_2$  as well as  $T_c^\infty$  to be basically stable whereas all the different coefficients  $\alpha_i$  may vary somewhat between different products, as they will depend upon the molar mass distribution and the co-unit distribution in the chains which often does not show an ideal randomness.

**Acknowledgements** Support of this work by the Deutsche Forschungsgemeinschaft (Sonderforschungsbereich 428) is gratefully acknowledged. Thanks are also due to the “Fonds der Chemischen Industrie” for financial help. T.Y. Cho is grateful for the support by the Ministry of Education of Korea in the “Brain Korea 21 Program” and for the sponsoring by LG Chemicals in the industrial-academic collaboration program.

## References

1. Hauser G, Schmidtke J, Strobl G (1998) *Macromolecules* 31:6250
2. Heck B, Hugel T, Iijima M, Sadiku E, Strobl G (1999) *New J Physics* 1:17
3. Strobl G (1970) *Acta Crystallogr* A26:367
4. Ruland W (1977) *Colloid Polym Sci* 255:417
5. Schmidtke J, Strobl G, Thurn-Albrecht T (1997) *Macromolecules* 30:5804
6. Wunderlich B (1980) *Macromolecular physics*. Academic Press, vol 3, p 58
7. Strobl G (2000) *Eur Phys J E* 3:165
8. Fougères C, Dosière M, Koch MHJ, Roovers J (1998) *Macromolecules* 31:6266
9. Robelin-Souffache E, Rault J (1989) *Macromolecules* 22:3582